

Self-assembly of Hydrophilic Gold Nanocrystals into Nanoparticle Crystals

Suhua Wang, Seiichi Sato, Keisaku Kimura*

Department of Material Science, Graduate School of Sciences, Himeji Institute of Technology, 3-2-1 Koto, Kamigori-Cho, Ako-Gun, Hyogo, 678-1297, Japan
Fax: 81-791-58-0161

The self-assembly of mercaptosuccinic acid (MSA)-coated Au nanocrystals 3.7 nm in diameter into nanoparticle crystals in bulk aqueous solution has been accomplished. The self-assembly is dependent on the pH value of the solution, and high quality nanoparticle crystals grow in a pH value range of 0.3-1.0. SEM observation shows that these nanoparticle crystals possess distinct shape, sharp facet features of quality crystals. Elemental analysis suggests the acidic form of the MSA molecules within the Au nanoparticle crystals. Small angle XRD and transmission electron diffraction (TED) cooperatively determine the hexagonal close packing (hcp) of Au nanoparticles in the nanoparticle crystals. The lattice fringe of the nanoparticle crystals is clearly observable using TEM and the fringe spacing is measured to be ~ 4.5 nm, which is consistent with that computed from a hcp stacking model.

Key words: nanoparticle crystals, self-assembly, superlattices, gold nanocrystals

1. INTRODUCTION

The self-assembly of nanoparticles into ordered two- or three-dimensional arrays, namely nanoparticle crystals or nanocrystal superlattices (NCSs) has recently been attracted much effort.¹⁻¹⁵ An important feature of the nanoparticle crystals is the double periodicity: the atomic periodicity in angstrom range and the superlattice periodicity in nanometer scale. The properties of such double periodical superstructures can be tailored in a subtle way than those of simple crystals or single nanoparticles by controlling the nanoparticle core size, chemical nature of coating organic ligands, and the arrangement of nanoparticles in the arrays. Furthermore, the nanoparticle crystals provide opportunities to investigate the collective properties different from individual nanoparticle and the coupling interaction between nanoparticles in the superlattices. Therefore, the self-assembly of nanoparticles into ordered arrays provides a route to new nanostructured materials with optimized and enhanced properties and future optical and electronic devices. Here we report the preparation and structural determination of faceted large gold nanoparticle crystals generated by homogeneous nucleation in the bulk aqueous solution.

2. EXPERIMENT

2.1 Preparation of MSA-coated Gold Nanoparticles

The MSA-coated gold nanoparticles were prepared using a procedure basically similar to that described in previous work¹⁶ but largely modified for mass production. Briefly, under vigorous stirring and ultrasonic irradiation 80 ml of freshly prepared 0.3M NaBH₄ aqueous solution was added to a water methanol mixture containing 1.0 g of

HAuCl₄·4H₂O and 0.73 g of MSA. After the reduction reaction, a flocculent precipitate was washed with water methanol mixture by repeating re-suspension and re-centrifugation processes, followed by dialyzing against the flow of distilled water. A powder product of 0.6 g was obtained through lyophilization and evacuating on a vacuum line. The mean diameter of the MSA-coated gold nanoparticles was determined to be 3.7 nm with fwhm of 0.5 nm using TEM, as shown in Fig. 1.

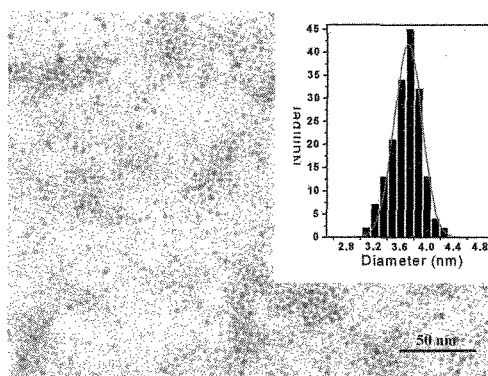


Fig.1 TEM image of the MSA-coated gold nanoparticles for self-assembly. The inset presents the particle size histogram of sample number 168.

2.2 Self-assembly of Gold Nanoparticles

7.2 mg of MSA-coated Au nanoparticle powder was dispersed in 4.0 ml of distilled water to form brown solutions, and the pH value of the dispersion was adjusted with 6.0M HCl aqueous solution. Then the solution sample was filtered through a syringe-driven micro-filter with 0.22- μ m pore immediately before they were stored in a sealed

glass vial. After 3-5 days under room temperature, the crystallization took place in a wide range of HCl concentration ($0.3 \pm 0.2M$) giving numerous faceted crystals with micrometer sizes. These gold nanoparticle crystals were transferred to silicon substrate before analysis.

3. RESULTS AND DISCUSSION

SEM image (Fig. 2) of the sample clearly shows that these as-prepared nanoparticle crystals possess distinct shape and sharp facet features of quality crystals. The vagueless and non-charging SEM

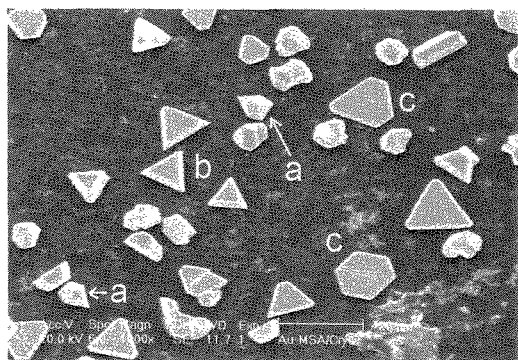


Fig. 2. SEM image of the faceted Au nanoparticle crystals prepared in bulk aqueous solution shows clear crystal habit.

images of the nanoparticle crystals imply that the Au nanoparticle crystals may be electrical conducting. The cross dimensions of the Au nanoparticle crystals are measured to be in the range of $\sim 6-15 \mu m$ and the thickness is estimated to be less than $5 \mu m$. The nanoparticle crystals exhibit a diversity of shapes. The majority is platelet crystals with triangular (labeled b) or hexagonal (labeled c) features. Some other gold nanoparticle crystals, however, have the diamond-like shapes such as those labeled 'a' in Fig. 2. The various shapes are developed when the growth rates in different directions of the crystals are different. In general, the growth rate in the direction normal to the top surface of the platelet crystals is slower than those in other directions. The elemental composition of these faceted crystals is qualitatively determined using Energy Dispersive X-ray spectroscopy (EDX). The EDX experiment is performed on each individual crystal possessing triangular, hexagonal, or diamond-like shape. The EDX results show that all crystals have the similar elemental composition of predominant Au component accompanied by some carbon, oxygen, and sulfur contents. The gold component and other components are attributed to the gold cores and MSA coating layers, respectively. The absence of sodium in the EDX spectrum suggests that the MSA molecules in the nanoparticle crystals be in the acidic states. This is reasonable because the self-assembly of MSA-coated gold nanoparticles was carried out in a relatively strong acidic media. This finding suggests hydrogen

bonding network amongst MSA molecules within the nanoparticle crystals.

To uniquely determine the crystallographic data of the Au nanoparticle crystals, small angle electron diffraction and X-ray diffraction experiment are carried out. Trace b in Fig. 3 shows the powder X-ray diffraction pattern in wide-angle range recorded from the nanoparticle crystals. X-ray diffraction peaks from atomic Au lattices of the nanoparticles are clearly seen. Trace a in Fig. 3 is recorded from the same nanoparticle crystal sample at small angles, and it is directly related to the ordered assembly of the nanoparticles. The small angle XRD pattern indicates a hexagonal-close or face-centered-cubic packing of the Au nanoparticles with diameter of 3.7 nm . The position marked with asterisk could not be associated with any diffraction from either hcp system or cubic-close-packing systems. This contribution may be attributed to a small amount of stacking faults in some nanoparticle crystals. The XRD pattern is successfully indexed as hexagonal close-packing of gold nanoparticle with the parameter of $a = 5.25 \text{ nm}$. The spacing between adjacent Au nanoparticle cores is computed based on the crystallography of the crystals to be 1.55 nm . It is reasonable if we consider that the thickness of MSA monolayer over the surface of Au core is $\sim 0.7 \text{ nm}$ ¹⁷ and these building units are assumed to be stacked in hexagonal close packing just like hard spheres. Selected area small angle transmission electron diffraction technique is adapted to collect further crystallographic data from nanoparticle crystals for structural determination. In order to

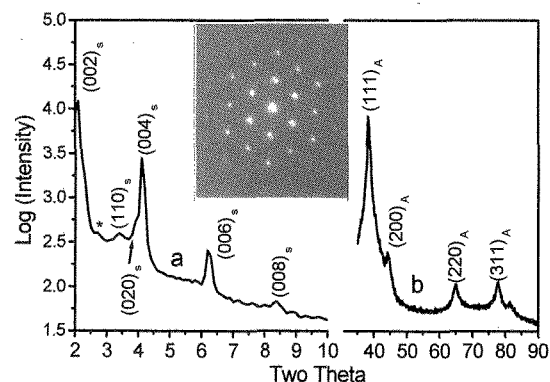


Fig. 3 XRD patterns recorded at a small angle range (a) and a wide angle range (b). The subscript S of the Miller indices means from the superlattice and subscript A means from the atomic lattice of Au nanoparticles. The inset is a representative of electron diffraction pattern recorded from an individual Au colloidal crystal with a camera length of 2.0 m .

obtain a statistical result, the selected area electron diffraction experiments are performed on randomly sampled individual nanoparticle crystals having triangular, hexagonal, or diamond-like

shapes. The electron diffraction experiment is unsuccessful on the crystals with diamond-like shape owing to their large thickness. But very clear electron diffraction patterns can be obtained from triangular-shaped or hexagonal-shaped platelet crystals. The TED patterns recorded from randomly sampled twelve crystals have the same pattern and inter-spot distance. The inset in Fig. 3 is a representative of transmission electron diffraction pattern of sharp spots, exhibiting six-fold symmetric arrangement. Clearly, the hexagonal pattern indicates six-fold projected symmetry in the nanoparticle crystals. By the combination of XRD data with TED data, the electron diffraction can only be indexed as the [0001] zone patterns of the hcp crystal structure system with the parameter of $a = 5.25$ nm. The hexagonal structure system can fit with the ED and XRD pattern completely and consistently. Therefore, the analysis and results suggest that the Au nanoparticles be uniquely stacked with hexagonal close packing in the nanoparticle crystals. It can be also seen from the diffraction pattern that even the third order diffraction spots are observable, suggesting the formation of perfect Au nanoparticle crystal on a large scale.

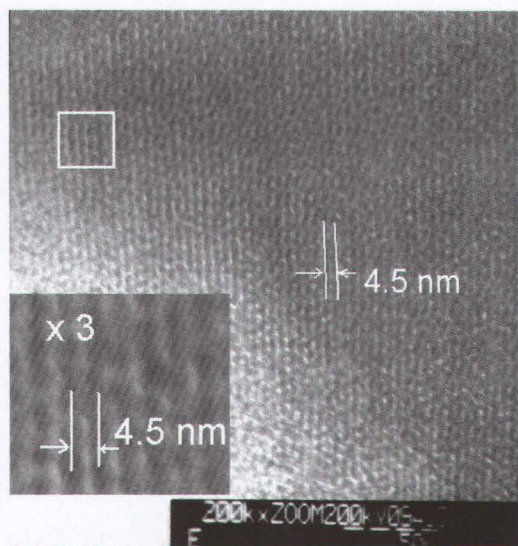


Fig.4 High resolution TEM image showing the superlattice fringes of {100} in the hcp system. The inset presents the enlargement of the boxed area.

High resolution TEM experiment is also carried out on the sample in order to observe the stacking behavior of Au nanoparticles within the nanoparticle crystals. Because of the thickness of the nanoparticle crystals, the superlattice fringes are only observable at the edge of the crystal. Fig. 4 presents the high resolution TEM image and the lattice fringes are clear. The fringe spacing is measured to be ~ 4.5 nm and is close to the d -spacing of the lattice planes with the type of $\{10\bar{1}0\}$ (4.55 nm) in hcp system, in agreement

with the primary diffraction of small angle TED.

On the basis of the above discussion and analysis, a stacking model can be drawn from the hexagonal close packing. For the stacking model the MSA-coated gold nanoparticles are treated as simple hard spheres. In the hexagonal close packing model of hard spheres the unit cell parameter a is equal to the distance between two adjacent spheres' centers. Fig. 5 depicts the stacking behavior of the hexagonally packed Au nanoparticles viewed along the [0001] zone axis of the crystal. For simplicity, only single layer of Au nanoparticles on the (0001) lattice plane is present. The thickness (0.85 nm) of the coating organic layer deduced from the stacking model is comparable to that reported (~ 0.7 nm). The deviation is acceptable since the thickness of the coating organic molecule is estimated grounded on the bond length. In addition, the error may be due to the simplicity of the Au nanoparticles' being treated as simple hard spheres. Considering the carboxyl group tail of the coating MSA molecule, it is reasonable to access that the adjacent Au nanoparticles are interconnected by hydrogen bonding either direct coupling amongst carboxyl

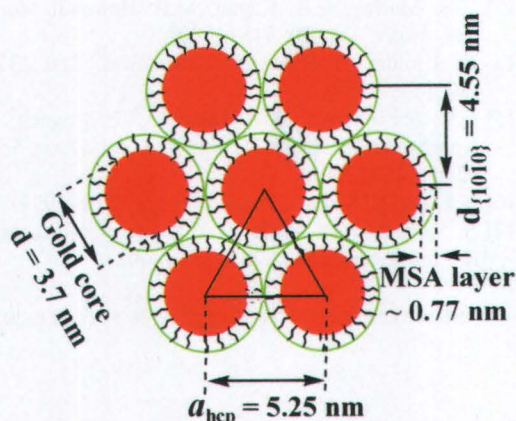


Fig. 5 The schematic showing the stacking model of Au nanoparticles viewed along the [0001] zone axis of the hcp system when the Au nanoparticles were treated as simple hard spheres.

groups or through water molecules. In the later case, the distances among adjacent Au nanoparticles are apparently expanded. The coupling interactions amongst building Au nanoparticle units in the nanoparticle crystals are interesting because they can affect not only the stacking behavior of particles, consequently affecting the final crystal structure but also the electronic properties of the nanoparticle crystals.

Acknowledgments. Financial support and granting the postdoctoral fellowship (P01261) of this work from the Japan Society for Promotion of Science is gratefully acknowledged. The authors are indebted to support in part by Grants-in-aid for Scientific Research (B:13440212) from Ministry of Education, Culture, Sports, Science and Technology.

Reference

- [1] C.B. Murray, C.R. Kagan, M.G. Bawendi, *Science*, **270**, 1335 (1995).
- [2] S.A. Harfenist, Z.L. Wang, M.M. Alvarez, I. Vezmar, R.L. Whetten, *J. Phys. Chem.*, **100**, 13904 (1996).
- [3] J. Fink, C.J. Kiely, D. Bethell, D.J. Schiffrin, *Chem. Mater.*, **10**, 922, (1998).
- [4] X.M. Lin, C.M. Sorensen, K.J. Klabunde, *Chem. Mater.*, **11**, 198, (1999).
- [5] J.E. Martin, J.P. Wilcoxon, J. Odinek, P. Provencio, *J. Phys. Chem. B*, **104**, 9475 (2000).
- [6] S.A. Harfenist, Z.L. Wang, R.L. Whetten, I. Vezmar, M.M. Alvarez, *Adv. Mater.*, **9**, 817 (1997).
- [7] Z.L. Wang, *Adv. Mater.*, **10**, 13 (1998).
- [8] H. Kang, Y.W. Jun, J.R. Park, K.B. Lee, J. Cheon, *Chem. Mater.*, **12**, 3530 (2000).
- [9] L. Motte, F. Billoudet, E. Lacaze, J. Douin, M.P. Pileni, *J. Phys. Chem. B*, **101**, 138 (1997).
- [10] C.P. Collier, T. Vossmeier, J.R. Heath, *Annu. Rev. Phys. Chem.* **49**, 371 (1998).
- [11] A. Taleb, V. Russier, A. Courty, M.P. Pileni, *Phys. Rev. B*, **59**, 13350 (1999).
- [12] S. Sun, C.B. Murray, *J. Appl. Phys.*, **85**, 4325 (1999).
- [13] C.B. Murray, C.R. Kagan, M.B. Bawendi, *Annu. Rev. Mater. Sci.*, **30**, 545 (2000).
- [14] K. Kimura, S. Sato, H. Yao, *Chem. Lett.*, 372, (2001).
- [15] E.V. Shevchenko, D.V. Talapin, A.L. Rogach, A. Kornowski, M. Haase, H. Weller, *J. Am. Chem. Soc.*, **124**, 11480 (2002).
- [16] S. Chen, K. Kimura, *Langmuir*, **15**, 1075 (1999).
- [17] S. Sato, N. Yamamoto, H. Yao, K. Kimura, *Mat. Res. Soc. Symp. Proc.*, **703**, 375 (2002).

(Received December 20, 2002; Accepted March 1, 2003)